

Research Article

Taxonomic and functional diversity of North American vegetation during the last interglacial–glacial cycle

Timothy Terlizzi^a and Thomas Minckley^{a,b}

^aDepartment of Geology & Geophysics, University of Wyoming, Laramie, WY, USA and ^bProgram in Ecology and Evolution, University of Wyoming, Laramie, WY, USA

Abstract

We synthesized pre-last glacial maximum pollen records to reconstruct North American pollen diversity since ca. 130 ka. Using taxonomic diversity (a measure of the number and abundance of taxa) and functional diversity (a measure of the number and abundance of different phenotypes) we identified temporal and spatial diversity trends for six North American bioregions: Arctic, Intermountain West, Mexico, Pacific Northwest, Southeast, and Yucatán. Reconstructed taxonomic temporal and spatial trends vary among bioregions, with regional diversity patterns captured in the functional metric, suggesting shifts in species composition coincide with shifts in ecosystem function. However, significant shifts in taxonomic pollen diversity differed in frequency, magnitude, and timing from their functional counterparts. Variations in both regional taxonomic and functional diversity response to global and regional temperature trends were evident, suggesting temperature alone does not fully explain changes in species composition. Regional richness estimates exhibited higher stability relative to the weighted diversity estimates indicating low levels of species turnover through Late Quaternary warming–cooling phases. Shifts in regional diversity did not predictably respond to stadial and interstadial transitions. Instead, North American patterns of plant diversity over the last ca. 130 ka differ geographically, likely responding to regional rather than global climate change.

Keywords: Quaternary; paleogeography; glaciation; North America; pollen; vegetation dynamics

Introduction

Studying past climatic variations to understand the processes that determine plant community composition and resilience to large-scale compositional shifts is central to paleoecology (Tausch et al., 1993; Willis et al., 2010; Birks, 2019). North American climate–vegetation relationships from the last glacial maximum (LGM) to the present are well explored (e.g., Bartlein et al., 1998; Williams et al., 2004). Longer timescale relationships, such as the conditions during the last interglacial–glacial cycle, are less known but do provide an opportunity to examine multiple examples of vegetation responses to climate shifts, such as those that occur between Marine Oxygen Isotope stages (MIS).

The last interglacial–glacial cycle (MIS 5–2) contains several warm (interstadial) and cold (stadial) periods useful for examining vegetation responses to rapid, global-climate shifts. Climate driven responses of vegetation have been explored using European pollen records (Guiot et al., 1993; Cheddadi et al., 2005; Lucchi, 2008; Jiménez-Moreno et al., 2010b), and regionally in North America (Glover et al., 2021). Compiling pre-LGM pollen records at continental scales provides both a novel dataset for paleoecological study and for reconstructing vegetation dynamics independent of human influence through multiple climate scenarios between stadial and interstadial periods (Tzedakis et al., 2009). European

records suggest MIS 5e was $>4.3^{\circ}\text{C}$ warmer than present with higher plant community turnover in Central Europe compared to the north and south (Wohlfarth, 2013; Felde et al., 2020; Wilcox et al., 2020). Europe transitioned between warm, forested periods during MIS 5 and cool, open vegetation from MIS 4 through MIS 2 (Helmens, 2014). In North America few syntheses of last interglacial–glacial vegetation changes exist, despite available data (Glover et al., 2021) (Table 1). Around 50 North American pollen records are reported to pre-date the LGM (Williams et al., 2018). Of these, ~ 20 have sampling-resolution and age-model constraints that allow for a pre-LGM analysis of continental-scale, temporal and spatial patterns of diversity change. These data are distributed across several North American ecoregions (Fig. 1). Grouping individual sites into broader ecoregions (Bailey, 2014) allows for an ecosystem-centric examination of vegetation dynamics for the past 130 ka.

Plant communities vary along environmental gradients at different spatial and temporal scales (ter Braak and Prentice, 2004). These often appear as elevational and latitudinal gradients that result from underlying temperature and moisture gradients, particularly in mountainous regions (Gentry, 1988; von Humboldt and Bonpland, 2010; Lamanna et al., 2014; Felde et al., 2016). As environmental gradients shift, the spatial extent of plant communities shift in response (Comes and Kadereit, 1998; Thuiller et al., 2005). Plant communities can be characterized through estimates of taxonomic diversity, incorporating measures of richness (number of taxa) and evenness (distribution of taxa abundances) (Schuler and Gillespie, 2000; Howard and Lee, 2003; Sax

Corresponding author: Thomas Minckley; Email: minckley@uwyo.edu

Cite this article: Terlizzi, T., Minckley, T., 2025. Taxonomic and functional diversity of North American vegetation during the last interglacial–glacial cycle. *Quaternary Research*, 1–15. <https://doi.org/10.1017/qua.2024.55>

Table 1. Table of sites used in this study and their associated publications. Age Range calculated as the difference between the youngest date and the oldest. Region includes the DCA-based grouping made in this study.

Region	Record Name	Longitude	Latitude	Age Range (cal yr BP)	Publications	Dataset DOI
Intermountain West	Baldwin Lake	-116.8064	34.2764	14,602–103,708	Glover et al., 2017, 2020	https://doi.org/10.21233/0A8S-FT20
Intermountain West	Bear Lake	-111.3330	41.9844	0–224,425	Colman et al., 2006; Jiménez-Moreno et al., 2007	https://doi.org/10.21233/qm0e-tv75
Intermountain West	Carp Lake	-120.8806	45.9181	0–133,899	Whitlock et al., 2000	https://doi.org/10.21233/n3597b
Mexico	Poza Tierra Blanca	-102.0000	26.0000	-68–84,814	Minckley et al., 2019	
Pacific Northwest	Fargher Pond	-122.5192	45.8868	18,756–58,513	Grigg & Whitlock, 2002	https://doi.org/10.21233/29yf-f996
Arctic	Fog Lake	-63.2495	67.1824	119–46,944	Wolfe et al., 2000; Miller et al., 2002; Fréchet et al., 2006, 2008	https://doi.org/10.21233/bqja-m092
Southeast	Goshen Springs	-86.1342	31.7211	0–54,999	Delcourt et al., 1980	https://doi.org/10.21233/n3604d
Pacific Northwest	Grass Lake	-122.1672	41.6496	459–35,477	Hakala & Adam, 2004	https://doi.org/10.21233/fvkb-9e77
Intermountain West	Gray Lake	-111.4380	43.0662	4,985–97,507	Beiswenger, 1991	https://doi.org/10.21233/fvhw-s571
Arctic	Hanging Lake	-138.3833	68.3833	0–41,138	Cwynar, 1982	https://doi.org/10.21233/n35s6s
Intermountain West	Hay Lake	-109.4250	34.0000	94–45,629	Jacobs, 1985	https://doi.org/10.21233/n38k71
Arctic	Joe Lake	-157.2167	66.7667	0–43,804	Anderson, 1988	https://doi.org/10.21233/n39t6c
Pacific Northwest	Kalaloch	-124.3830	47.6342	17,088–67,200	Heusser, 1972	https://doi.org/10.21233/MV7N-E893
Intermountain West	Last Canyon Cave	-108.3948	45.0956	12,885–48,558	Minckley et al., 2021	
Pacific Northwest	Little Lake	-123.5840	44.1666	243–40,566	Worona & Whitlock, 1995	https://doi.org/10.21233/n3ff1x
Intermountain West	Natural Trap Cave	-108.1930	44.9733	0–150,652	Minckley et al., 2023	
Mexico	Lake Patzcuaro	-101.5833	19.5833	20–44,100	Watts & Bradbury, 1982	https://doi.org/10.21233/n3bj2d
Yucatán	Lake Petén-Itzá	-89.8419	16.9640	40–85,408	Correa-Metrio et al., 2012a, b	https://doi.org/10.21233/dmvc-9j61
Intermountain West	Ruby Marsh	-115.5049	41.1340	0–34,601	Thompson, 1992	https://doi.org/10.21233/d01t-8d61
Intermountain West	Star Meadows	-114.6837	46.5166	-60–125,223	Herring & Gavin, 2015	https://doi.org/10.21233/8fsd-4z98
Mexico	Gulf of Tehuantepec (ME0005A 11PC)	-95.2920	15.7133	1,755–28,798	Hendy et al., 2016	
Southeast	Lake Tulane	-81.5034	27.5861	-7–51,979	Grimm et al., 2006	https://doi.org/10.21233/n30b5c
Arctic	Zagoskin Lake	-162.1084	63.4485	47–36,790	Ager, 2003	https://doi.org/10.21233/6pz8-g423

and Gaines, 2003). Studies show high plant diversity maintains ecosystem functions and services including high net primary productivity (NPP) (Tilman et al., 1997; Hector et al., 1999; Isbell et al., 2011). High diversity is supported by biotic and abiotic factors that allow for independent regional responses to climate (Zak et al.,

2003; Benton, 2009; López-Angulo et al., 2020). Understanding how plant communities respond to shifts in climate in addition to the conditions that support high diversity can help predict the effect of current warming on ecosystems as they adapt (Stohlgren et al., 2000; Suggitt et al., 2019).

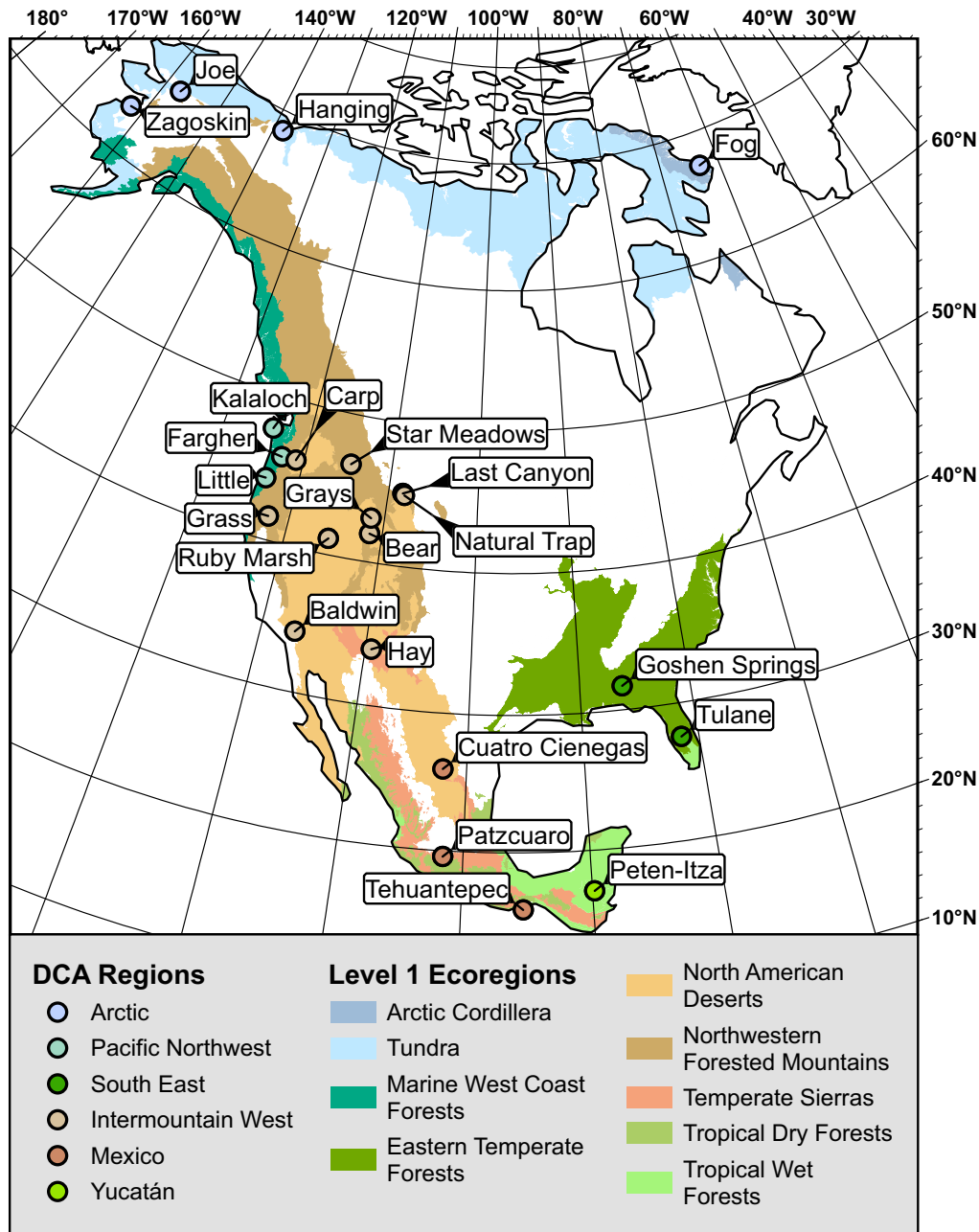


Figure 1. Map of the 23 sites used in this study. Site locations are shown as circles with the site names. Sites are colored based on the seven regional groupings determined by the DCA (Supplemental Figure 2). The seven DCA regions encompass nine level-I ecoregions. The represented ecoregions are shown in color and listed in the legend. Several of the seven DCA regions represent multiple level ecoregions. Due to the lack of sites in the northeast, the Eastern Temperate Forest is divided into level-II classifications.

Reconstructions of pollen-based, paleodiversity provide scenarios to study shifts in plant community composition (Birks, 2019). Modern pollen-derived taxonomic diversity estimates have effectively captured the structure and composition of vegetation on landscapes at local scales (van der Knaap, 2009; Matthias et al., 2015; Birks et al., 2016; Felde et al., 2016) and, while caution must be taken in interpreting pollen-derived diversity estimates (Weng et al., 2006; Goring et al., 2013; Väli et al., 2022), diversity estimates can address questions of diversity change from the trends produced. By reconstructing plant paleodiversity trends across North America, we can interpret both ecosystem diversity and dynamics as they responded to past climate changes.

Paleodiversity has been reconstructed via several common indices, including species richness, Shannon's index, and Simpson's index (Morris et al., 2014). While these methods are still commonly used, other methods such as Hill numbers are more versatile via their ability to vary between different orders (Jost 2006, 2007). Applying diversity indices in a paleo context can be complicated by several taxonomic-scale-related problems (Cleal et al., 2021), such as varying taxonomic resolution (Birks and Birks, 2000) and less information for taxonomic classifications (Godfray et al., 2004). While much of this is simply the nature of working within the fossil record, incorporating plant functional traits can provide a means to reconstruct ecosystem dynamics where taxonomy alone cannot

(Eronen et al., 2010; Barnosky et al., 2017; Chacón-Labela et al., 2023).

In this study, we used pollen-derived taxonomic and functional diversity estimates to quantify North American plant community dynamics from the last interglacial period (MIS 5e) to the present (MIS 1). We hypothesize that global temperature variability and latitudinal temperature gradient compression drove shifts in taxonomic and functional diversity. We examine whether continental and regional shifts in pollen-derived taxonomic diversity are mirrored in functional trait-based diversity for six geographic regions of North America based on 23 fossil pollen records.

Regional Setting

Modern North American ecoregion floristics are represented by high species richness in the tropics of southern Mexico, southeastern United States, and Pacific coast (Ricketts et al., 1999). We can use sub-biome ecoregions (Bailey, 2014) to characterize sub-continental scale regions with similar floristics to scale up from individual sites to broader, floristic heterogeneity at the continental scale. Richness is lowest in the sagebrush steppe and grasslands of the continental interior and Arctic tundra (Cavender-Bares et al., 2020). While plant and pollen diversity are not directly analogous, regional correlations between the two have been established in northern Europe (Reitalu et al., 2019).

To verify whether North American ecoregions reasonably correspond to the pollen record, we grouped 23 North American pollen records, dated to at least 40 cal ka BP, into six regions based on a detrended correspondence analysis (DCA) of pollen type abundances (Supplemental Figs. 1 and 2). These DCA-based groupings align with level-I ecoregions of North and Central America with 9 of 15 represented (Fig. 1) (CEC, 1997; Griffith et al., 1998). DCA clusters grouped similar pollen records based on floristic history rather than modern composition while still being recognizable within modern North American floristics. DCA clusters aligned with ecoregion determinations (CEC, 1997; Griffith et al., 1998), which allowed us to use ecoregion changes from present as an interpretive framework (Fig. 1).

Methods

The overall workflow is outlined in Fig. 2 with each step pertaining to one of three categories: data compilation, in which the datasets used were established, data preparation, in which data were transformed and filtered, and data analysis, in which data were used to generate the results presented.

Records selection

Published pollen data within North America with dated materials to at least 25 cal ka BP and extrapolated to at least 40 cal ka BP were compiled from the Neotoma Paleocology Database (Williams et al., 2018). Of the 28 records, three were removed for low resolution (fewer than 10 pollen samples or with data spanning less than 10 ka) and six were removed based on constraints in extrapolated age-depth models. Accepted sites also had extrapolations that followed reasonable sedimentation rates based on their 20–30 ka dated intervals. Four newer records not archived in Neotoma at the time of our study were included for a total of 23 records (Table 1). Raw pollen counts were available for all records used in this study.

Data conversions

Pollen taxa identified in each record were filtered based on the level of specificity of the identification. Only terrestrial pollen data were used, excluding spores, aquatic pollen types, and non-pollen palynomorphs to minimize site specific variability (e.g., wetland changes). Pollen taxa with less than 1% abundance in an individual record were excluded. Filtering identified pollen types reduced overall pollen-based, taxonomic richness, but aided in reducing researcher specific biases in pollen identification. The resulting data set contained 142 total pollen types, with 39 family-, 96 genus-, and 7 species-level pollen identifications (Supplemental Table 1).

We interpolated each record to address issues of radiometric dating. Raw pollen counts from each record were converted into relative proportions of the total terrestrial pollen and interpolated using a moving window weighted means interpolation to 1000-year time steps between 0 and 150 ka. Weighted mean interpolations of pollen data were ignored if temporal gaps within the original datasets exceeded ± 5 ka of the centroid of the targeted, 1000-year time step, resulting in discontinuities in our records. Samples within the ± 5 ka window were weighted using a normal curve based on their proximity to the centroid.

DCA and region determination

Similarities of the ecological and taxonomic clustering of the 23 pollen records were verified using DCA, an ordination method appropriate for grouping proportional datasets distributed along broad environmental gradients (Holland, 2008; Oksanen et al., 2013). DCA was conducted on all samples from all records ensuring that complete histories were considered simultaneously. Other ordination approaches for determining pollen–environment relationships (e.g., canonical correspondence analysis [CCA]) did not improve or enhance our analysis.

Hill numbers

Hill numbers are a family of interrelated diversity estimates that vary by the weights of rare and common taxa and are expressed as ‘effective number of species’ (Chao et al., 2014a, b). Hill numbers have proven to be a versatile approach to representing multiple diversity estimates simultaneously (Ohlmann et al., 2019). While commonly used to represent taxonomic diversity, a framework exists for calculating functional diversity with Hill numbers, although it has yet to be adopted in a paleoecological context (Chiu and Chao, 2014). With taxonomic Hill numbers, the ‘species’ that diversity is calculated from is the relative proportion of the taxa. In functional Hill numbers, the ‘species’ is the functional distance between two taxa rather than the proportions (Chao et al., 2014a). Simply, the outputs of taxonomic Hill numbers are in units of ‘effective number of species’, indicating a value of x is equivalent to x number of equally abundant species within a community. Functional diversity is interpreted as x number of equally abundant and functionally distinct species.

Varying both taxonomic and functional Hill numbers by the variable q adjusts the weights between rare and common taxa or functional distances in an assemblage. Lower q values produce higher diversity estimates through the inclusion of both rare and common taxa/distances while higher q values produce lower estimates by filtering out rare taxa/distances. We calculated three taxonomic and three functional Hill numbers for each sample

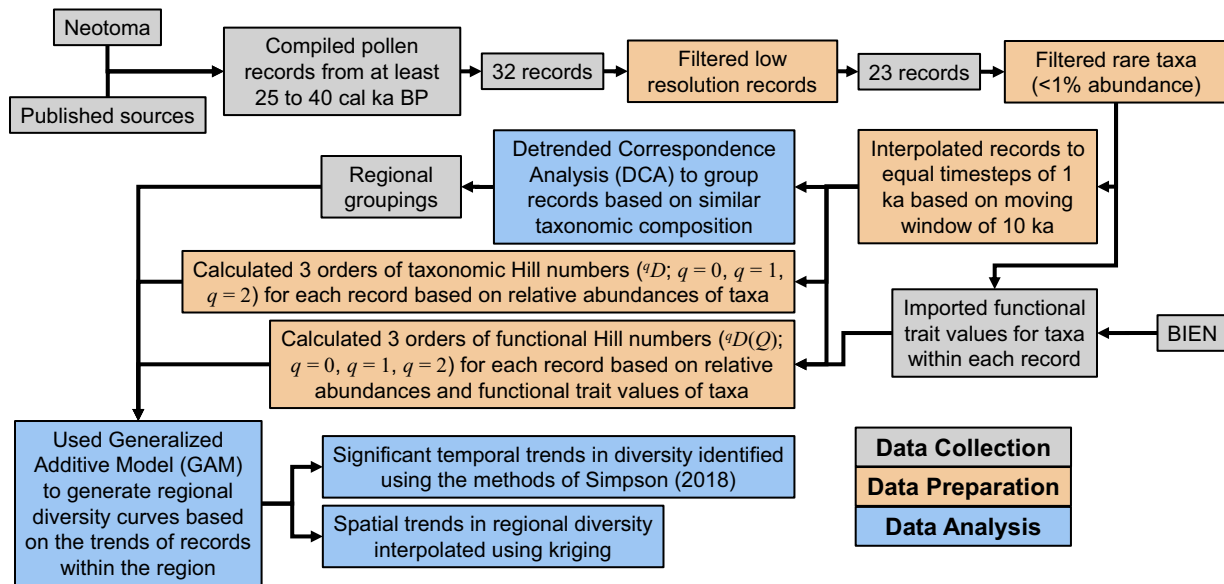


Figure 2. Flowchart of the workflow to generate taxonomic and functional diversity trends for the six regions in this study using publicly available datasets. Steps are colored based on three categories: data collection (gray), where data for the study were accessed; data preparation (orange), where data were filtered and transformed; and data analysis (blue), where the data presented in this study were created.

within a site to model diversity over time within the sites. The taxonomic Hill number of order q (qD) follow formula Equation 1a (Chao et al., 2014b):

$${}^qD = \left(\sum_{i=1}^S p_i^q \right)^{\frac{1}{1-q}} \quad (1a)$$

Where S equals the total number of species in the assemblage, p_i equals the proportion of species i . To represent functional diversity, Chiu and Chao (2014) modified taxonomic Hill numbers (qD) to include the mean functional distance between any two randomly sampled individuals in the assemblage using Rao’s quadratic entropy (Q) as defined by Equation 2 (Rao, 1982):

$$Q = \sum_{i=1}^S \sum_{j=1}^S d_{ij} p_i p_j \quad (2)$$

Where S and p_i remain unchanged from Equation 1a, p_j equals the proportions of species j , and d_{ij} equals the functional distance between species i and j , calculated using Gower distances. Distance measures are calculated between all species but vary in precision based on the number of trait observations. The resulting functional Hill numbers (${}^qD(Q)$) are described by Equation 3a (Chiu and Chao, 2014):

$${}^qD(Q) = \left[\sum_{i=1}^S \sum_{j=1}^S \frac{d_{ij}}{Q} (p_i p_j)^q \right]^{\frac{1}{2(1-q)}} \quad (3a)$$

Where all variables are the same as defined in Equations 1a and 2. When $q = 1$ in either metric, the equations are undefined and Equations 1b and 3b, which are equivalent to the limit as q approaches 1, must be used for taxonomic and functional diversity, respectively:

$${}^1D = \lim_{q \rightarrow 1} {}^qD = \exp \left(- \sum_{i=1}^S p_i \log p_i \right) \quad (1b)$$

$${}^1D(Q) = \lim_{q \rightarrow 1} {}^qD(Q) = \exp \left[- \frac{1}{2} \sum_{i=1}^S \sum_{j=1}^S \frac{d_{ij}}{Q} p_i p_j \log (p_i p_j) \right] \quad (3b)$$

The first three orders of taxonomic diversity collapse down to three common indices: Richness (0D), Shannon’s index (1D), and Simpson’s index (2D). These indices weight all species equally, all species by their relative abundance, and all species by the square of their relative abundance, respectively. For functional diversity, ${}^0D(Q)$ and ${}^2D(Q)$ correspond to functional attribute diversity (FAD) and Gini–Simpson index. ${}^1D(Q)$ does not correspond to an existing index, but for naming consistency we refer to it as functional Shannon’s index, although it is important to reiterate the two are not directly equivalent (Chiu and Chao, 2014). ${}^0D(Q)$ can be thought of as the sum of all functional distances, ${}^1D(Q)$ as the sum of all functional distances weighted by their relative abundance, and ${}^2D(Q)$ as the sum of all functional distances weighted by the square of their relative abundance.

Seven traits were selected for functional diversity analysis: leaf mass per area, leaf lifespan, max plant height, max plant longevity, seed mass, whole plant growth form, and whole plant woodiness. We selected these traits due to their abundant number of observations and ability to represent most plant ecological strategies through the leaf–height–seed scheme (Westoby, 1998). Some traits are auto-correlated (e.g., leaf lifespan and leaf mass per area), affecting d_{ij} and Q , which in turn alter the magnitude of functional diversity values, but not the overall pattern, which is driven by p_i and p_j .

Trait data were compiled following Brussel and Brewer (2021), using the Botanical Information and Ecology Network (BIEN) database and filtered to include only North and Central America taxa (Maitner et al., 2018). For species-level pollen-types, trait values for all occurrences were averaged and reported. For genus- or family-level pollen types, we averaged the values of all species in those groupings and used the averages as the trait value for

the taxon. Families and genera containing species with multiple growth forms (herbaceous and woody taxa) were treated as a different category from woody or herbaceous taxa when calculating functional diversity. To quantify the uncertainty associated with using trait averages, we performed a Monte Carlo simulation. Trait values were resampled to create simulated distributions of 5000 values from which we calculated the mean. This was repeated 10,000 times, creating a distribution of 10,000 means per trait, from which we sampled 100 means and calculated the associated functional diversity estimates.

Distances are calculated from the trait values of each species compared pairwise with all other species in the assemblage. This method is effective in cases when all taxa within an assemblage are identified to the species level and there is little variation in trait values (Pérez-Harguindeguy et al., 2016). Complications arise when taxa within an assemblage are identified at genus or family levels and there is higher variation in trait values. Averaged trait values ignore the natural variability that exists within a genus or family (Roscher et al., 2018; Sotomayor et al., 2022). However, our goal is to use traits to group pollen (plants) independently of their underlying taxonomy rather than use traits for their functional interpretations. The resulting functional diversity estimate loses the ability to draw specific environmental interpretations but provides comparator diversity datasets to analyze along with taxonomic diversity data.

Temporal analysis

Regional diversity trends were interpolated using a generalized additive model (GAM) to smooth the individual trends of each site within a region. The GAM model was calculated using the 'gam' function within the mgcv package in R Studio (Wood, 2001). Age was used as the predictor and diversity as the response with a Gaussian family, a normal/identity link function, and a restricted maximum likelihood (REML) smoothing method. Records within each region vary in length, affecting the GAM smoother and decreasing individual site influence towards the present. We selected a GAM to allow for the identification of significant shifts in the diversity time series based on the methods outlined in Simpson (2018). Times of significant change were highlighted on the splines. Site diversity values were normalized around the mean to enable comparisons of shift magnitude between regions and to highlight differences between the temporal patterns of the taxonomic and functional metrics. Without normalization, questions of the validity of diversity estimate values could prevent thorough interrogations of the trends being presented. Raw diversity trends are shown in Fig 6 and Supplemental Figs 3, 4, and 5. GAM splines are plotted alongside regional temperature records ($\delta^{18}\text{O}$) and atmospheric CO_2 .

Spatial analysis

For each region, we calculated the average of non-transformed taxonomic and functional diversity of each MIS. We then interpolated average diversity using empirical Bayesian kriging, chosen for its ability to quantify standard error and assumption of spatial correlation between inputs (Krivoruchko, 2012). Resulting maps use a bivariate color scale in which high values in both taxonomic and functional diversity are displayed in blue and high values in either taxonomic or functional diversity are displayed in black or orange,

respectively. Results for each region are mapped to indicate the distribution of and change in diversity between MISs.

Results

Regionalization of records

Pollen records were grouped into six North American ecoregions: the Arctic (4 sites), Pacific Northwest (3 sites), Intermountain West (10 sites), the Southeast (2 sites), Mexico (3 sites), and Yucatán (1 site). The Yucatán site was an outlier in the DCA (Supplemental Figs. 1 and 2). The floristic composition of the Yucatán record is primarily tropical taxa, distinguishing it from all other records.

Temporal diversity trends

Monte Carlo simulations show minimal variation in the magnitude and no variation in the trend of functional diversity, indicating the estimates do not vary significantly with uncertainty in trait averages. We found trends for richness (0D) and FAD (${}^0D(Q)$) to be distinct from the trends for Shannon's (1D) and functional Shannon's indices (${}^1D(Q)$) and Simpson's (2D) and Gini-Simpson's indices (${}^2D(Q)$), while the trends of the latter two are similar. Richness and FAD are distinct from the other two orders because of its exclusion of abundance (Fig. 3). In most cases, trends for Simpson's and Gini Simpson's indices have steeper increases and decreases, appearing as Shannon's and functional Shannon's indices trends with higher amplitude (Figs. 4 and 5). In all three orders of q , diversity trends differ by region. Although continental-scale patterns of diversity change are not apparent, regional diversity show examples of long-term trends and the influence of stadial and interstadial periods.

Richness (0D) and FAD (${}^0D(Q)$) trends follow each other well with significant shifts in one commonly reflected in the other. Both metrics remains stable around the mean in all regions except Mexico. Richness trends in Mexico show relative increases, with below average richness at the beginning of the record and average richness by the end. All other regions fluctuate around the mean but do not exhibit long-term shifts in magnitude. Richness and FAD vary inconsistently from global temperature as represented by atmospheric CO_2 with regions responding independently and within region responses being unpredictable during stadial and interstadial conditions. Regional climate records align more closely with richness and FAD however there remains are large degree of variance in response to shifts in regional climate.

Shannon's (1D) and functional Shannon's indices (${}^1D(Q)$) trends are similar showing less stability around the mean than richness and FAD. Multiple regions fluctuate around the mean (e.g., Arctic, Pacific Northwest, Intermountain West, and Mexico), while others decrease (e.g., Southeast) or experience large shifts in diversity (e.g., Yucatán). Shannon's and functional Shannon's indices follow similar patterns to richness and FAD when compared with the regional climate records and atmospheric CO_2 . However, shifts in regional climate correspond more consistently with shifts in the Shannon's and functional Shannon's indices than with richness and FAD.

Simpson's (2D) and Gini-Simpson's indices (${}^2D(Q)$) trends again follow each other at a similar level to Shannon's and functional Shannon's indices. However, the two metrics mismatch to a higher degree in Mexico and the Arctic. Within

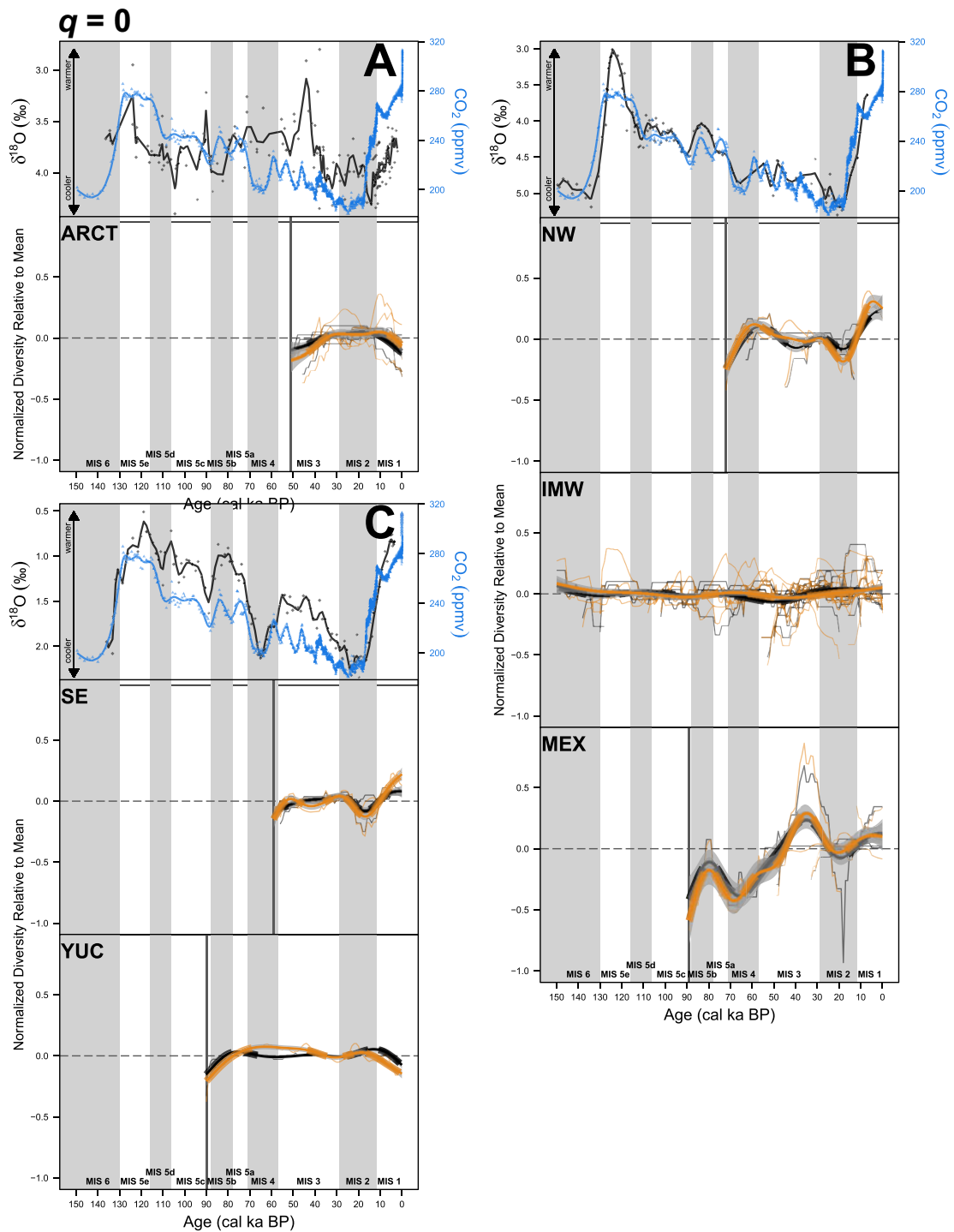


Figure 3. Normalized regional plant diversity of order $q = 0$ time series with climate. (A) Oxygen isotope record for the Arctic (Cronin et al., 2019) with arctic (ARCT) regional plant diversity. (B) Oxygen isotope record the Eastern Pacific Ocean (Herbert et al., 2001) with Pacific Northwest (NW), Intermountain West (IMW), and Mexico (MEX) regional plant diversity. (C) Oxygen isotope record for the Caribbean (Schmidt et al., 2004) with Southeast (SE) and Yucatán (YUC) regional plant diversity. Global atmospheric CO_2 concentration from the EPICA Dome ice core (Bereiter et al., 2015) is plotted in all climate plots in blue. Taxonomic richness (0D) is shown in black. Functional attribute diversity (FAD; ${}^0D(Q)$) is shown in orange. Individual site trends are plotted as thin lines. Gray vertical bars represent stadal (cool) MIS and white bars represent interstadial (warm) MIS (Lisiecki and Raymo, 2005). The dotted line at $y = 0$ indicates the mean of each site following normalization. Bold lines represent GAM splines displaying the interpolated diversity of order $q = 0$ trends for each region with the 95% confidence interval shaded. Thickened segments of the spline indicate sections of significant slope.

these two regions, Gini–Simpson’s index (${}^2D(Q)$) still has the same general pattern as Simpson’s index (2D), but there are differences in magnitude and timing of the shifts within the

patterns. Simpson’s and Gini–Simpson’s indices show nearly identical patterns of diversity shifts as Shannon’s and functional Shannon’s indices, differing only in magnitude, mirroring

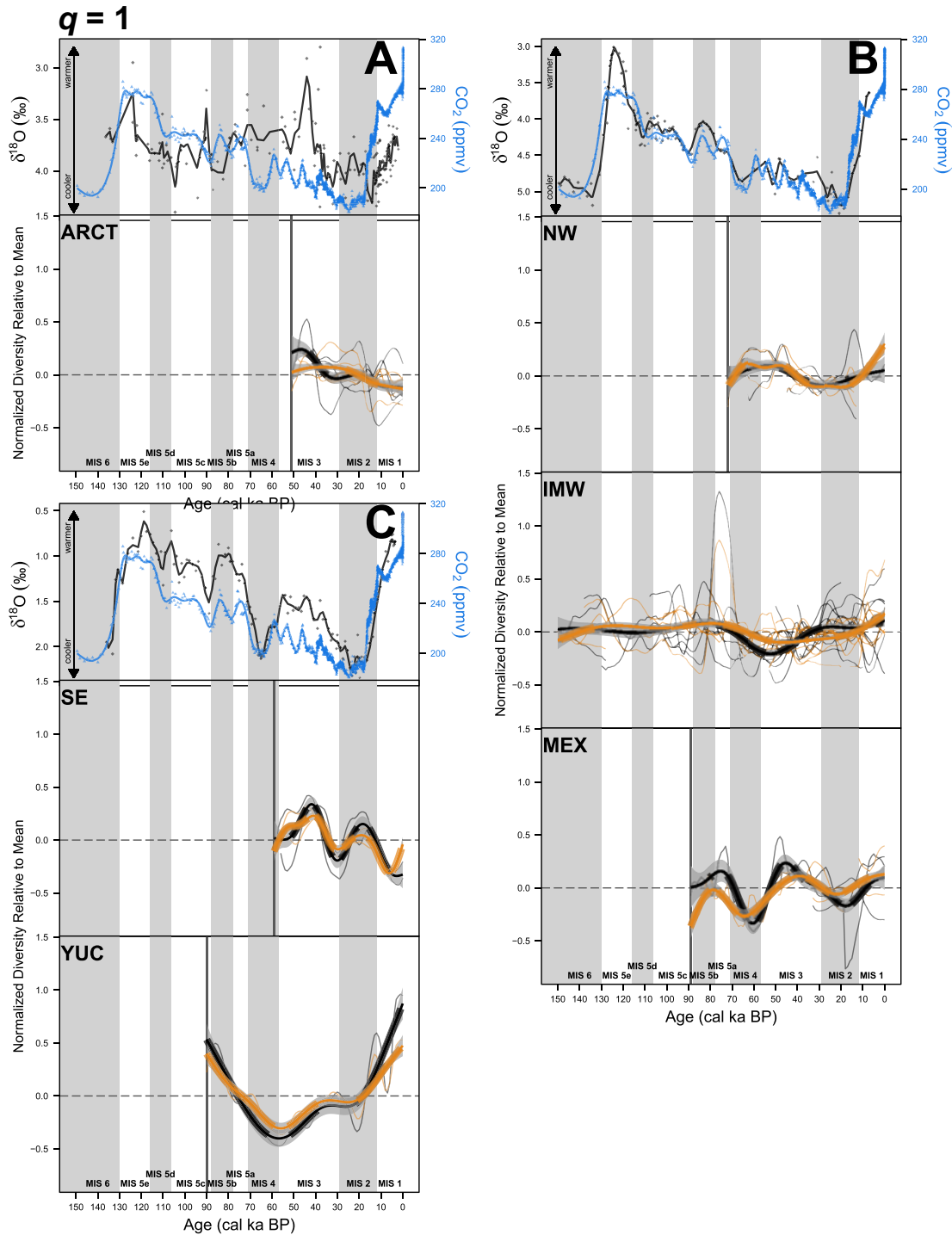


Figure 4. Normalized regional plant diversity of order $q = 1$ time series with climate following the format of Fig 3. Shannon's index (1D) is shown in black. Functional Shannon's index (${}^1D(Q)$) is shown in orange. ARCT = Arctic; NW = Pacific Northwest; IMW = Intermountain West; MEX = Mexico; SE = Southeast; YUC = Yucatán.

the atmospheric CO_2 and regional climate patterns previously described.

Geographic diversity distribution

Taxonomic (qD) and functional diversity (${}^qD(Q)$) align in terms of the geographic distribution of high and low regional diversity (Fig. 6). However, anticipated continental gradients from low- to

high-diversity regions are not consistent between the two metrics (e.g., Lamanna et al., 2014). Variation in the spatial extent of low taxonomic or functional diversity was not consistent continent-wide. Overall, eastern paleoecological records indicate higher taxonomic pollen diversity compared to western North America. North-south patterns show the Yucatán Peninsula exhibiting the highest diversity in all three orders of q . Prior to MIS 2, the Pacific Northwest shows similarly high diversity to the

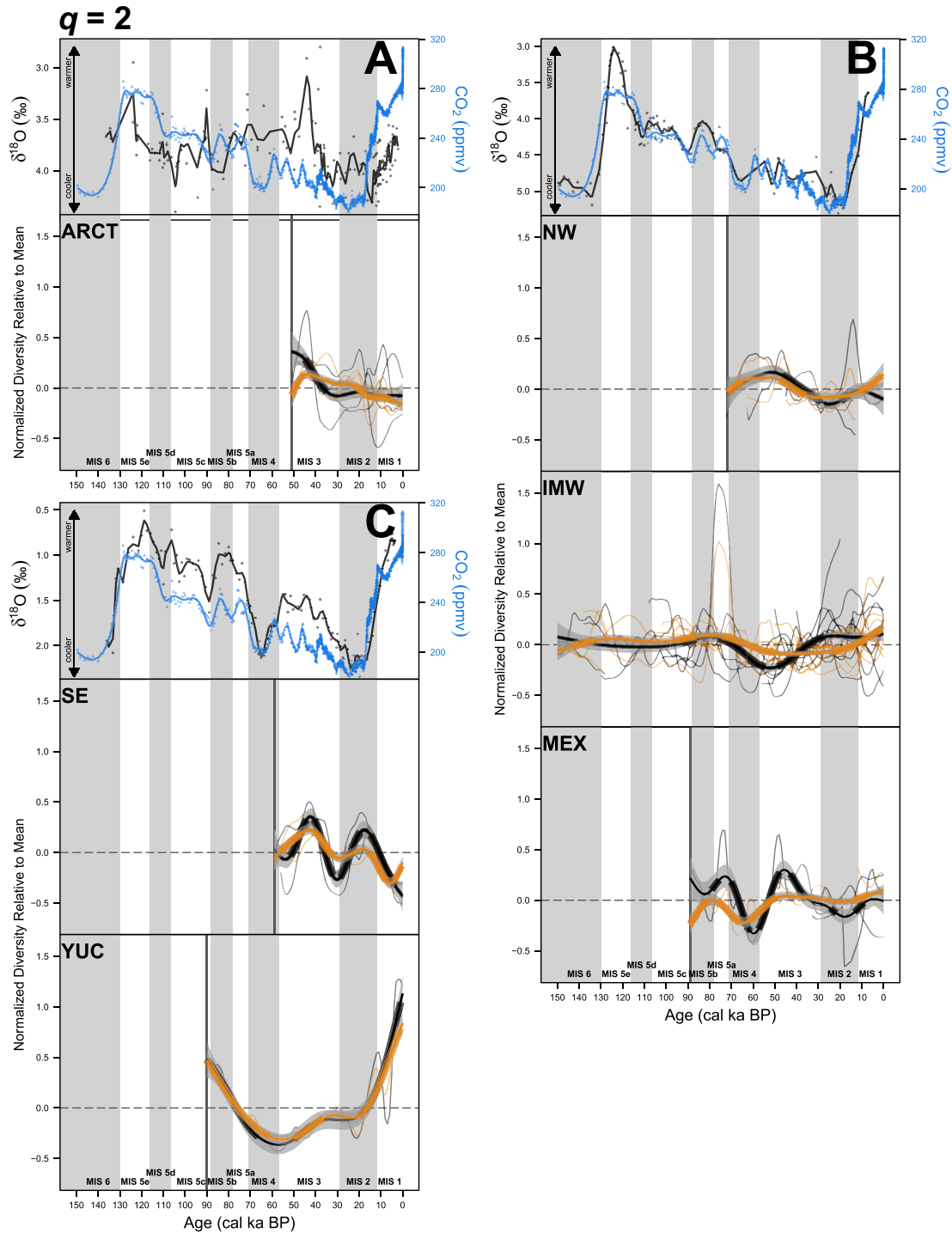


Figure 5. Normalized regional plant diversity of order $q = 2$ time series with climate following the format of Fig 3. Simpson's index (2D) is shown in black. Gini-Simpson's index (${}^2D(Q)$) is shown in orange. ARCT = Arctic; NW = Pacific Northwest; IMW = Intermountain West; MEX = Mexico; SE = Southeast; YUC = Yucatán.

Yucatán followed by the Southeast. These patterns of taxonomic pollen diversity are generally captured by the functional metrics with variance in the magnitude of functional diversity relative to taxonomic diversity.

Discussion

North American plant taxonomic and functional diversity underwent several asynchronous changes in the last ca. 130 ka.

We reject our hypothesis that global temperature variability and latitudinal temperature gradient compression drove shifts in taxonomic and functional diversity. Other global mechanisms, such as CO_2 variability, also do not appear to be drivers (Figs. 3–5). Changes in moisture flux into North America could explain regional diversity changes through the last interglacial–glacial cycle, but independent region-to-continental precipitation reconstructions are not available for comparison for this time period. Punctuated patterns of cooling and warming over

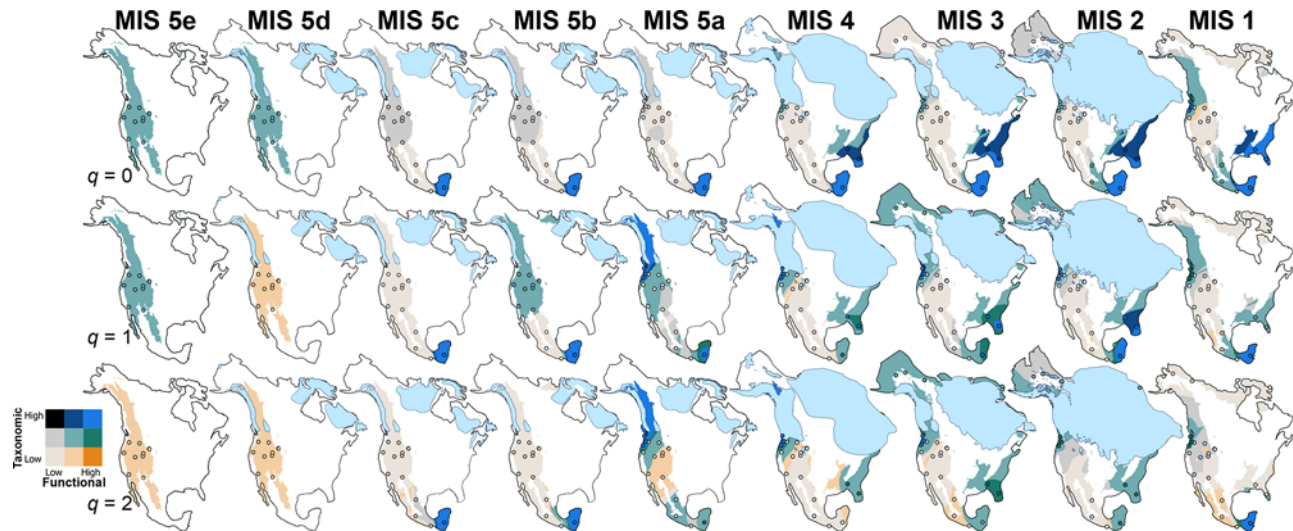


Figure 6. Bivariate maps of the geographic distribution of plant diversity in North America. Taxonomic diversity is indicated by the gray shading while functional diversity is orange shading. High values are indicated by dark shading and low values by light shading. Blue shading indicates overlap between taxonomic and functional diversity. Site locations are indicated by points colored by interpolation input values. Mismatches between site color and interpolated diversity are due to a combination of interpolation, including diversity of adjacent regions and the rounding of values. Ecoregions lacking data are overlain in white. Color schemes for both taxonomic and functional diversity are geometrically scaled (color intervals are based off a geometric series). Taxonomic richness (0D) is scaled from [minimum value – 17.9|17.9 – 24.6|24.6 – maximum value]. Functional attribute diversity (${}^0D(Q)$) is scaled from [minimum value – 25.2|25.2 – 34.0|34.0 – maximum value]. Shannon's index (1D) is scaled from [minimum value – 4.8|4.8 – 6.6|6.6 – maximum value]. Functional Shannon's index (${}^1D(Q)$) is scaled from [minimum value – 7.3|7.3 – 9.2|9.2 – maximum value]. Simpson's index (2D) is scaled from [minimum value – 3.3|3.3 – 4.7|4.7 – maximum value]. Gini-Simpson's index (${}^2D(Q)$) is scaled from [minimum value – 5.0|5.0 – 6.0|6.0 – maximum value]. The extent of the Laurentide Ice Sheet is shown in light blue (Batchelor et al., 2019). Continent coastlines based on the reconstructed sea-level trends from Cutler et al. (2003).

the last 130 ka did not consistently correspond to changes in taxonomic or functional diversity. When significant diversity changes occurred, we note misalignments in the temporal range between taxonomic and functional trends. With few exceptions, the trends for taxonomic pollen and functional diversity are similar, suggesting that these diversity calculations may be interchangeable.

Richness versus diversity

The trends for richness (0D) and FAD (${}^0D(Q)$) in each region are generally more stable than the trends for both Shannon's (1D) and functional Shannon's indices (${}^1D(Q)$) and Simpson's (2D) and Gini-Simpson's indices (${}^2D(Q)$). Many regions experience periods of significant change in richness and FAD, but significant changes are less frequent and smaller compared to diversity orders of $q = 1$ and $q = 2$, likely reflecting low regional species turnover over time. The pattern of significant change is consistent with species introductions and extirpations that require larger environmental shifts to change plant composition (Dakos et al., 2019). The assumption of an individualistic response to climate in paleoecological records is critical and implicitly includes other abiotic and biotic interactions, such as soil or competition conditions (Bartlein et al., 1986; Davis and Shaw, 2001). While difficult to quantify, it is possible that changes in richness and FAD require larger magnitude environment changes than are required to shift diversity orders of $q = 1$ and $q = 2$, particularly on millennial time scales if extirpation and immigration rates are equal. This is specifically true with pollen data where 'extirpation' of a pollen type must overcome local presence and potential residual long-distance transport from extra-local populations.

Diversity patterns of the entire community (order of $q = 1$) and the dominant taxa (order of $q = 2$) are similar, indicating

diversity shifts are occurring evenly throughout different floristic communities. Compared to richness (0D) and FAD (${}^0D(Q)$), Shannon's (1D), functional Shannon's (${}^1D(Q)$), Simpson's (2D), and Gini-Simpson's (${}^2D(Q)$) indices all experience higher degrees of diversity fluctuations (Figs. 3–5). These fluctuations indicate regional community composition varies while large species turnover is uncommon as indicated by the richness stability. Shifts in richness indicate extirpation and immigration as species ranges change. Our results show that the composition of floristic communities across the continent have been pliable in response to regional climate change.

Taxonomic versus functional diversity

Taxonomic and functional diversity trends are similar over the last ca. 130 ka, indicating paired analysis is not necessary if taxonomic or functional data are available. The two metrics differ in two key ways: when significant shifts occur in the time-series and the amplitude of trends. The use of Hill numbers allows us to be confident that similarities and differences between the metrics are a result of data differences and not an artifact of the selected indices. Differences between the two metrics could be due to shifts in the dominant plant functional types without corresponding shifts to the actual taxa present in these ecosystems (Doxa et al., 2020). For example, it's possible that with expansion of the Laurentide Ice Sheet, the southward displacement of conifers shifted the functional diversity in many regions that were previously dominant in broad-leaved trees (Williams et al., 2004).

Both taxonomic (qD) and functional (${}^qD(Q)$) metrics follow similar temporal and spatial patterns (Figs. 3–6), with both metrics capturing similar patterns of plant diversity across the continent. The similar overall patterns point to taxonomic and functional diversity being inherently linked. Ecosystems are high or low in

both metrics with mismatches uncommon (Fig. 6). Similarities between the two metrics show reconstructions of high taxonomic diversity can be considered as productive ecosystems without the need for functional diversity reconstructions. Some communities may experience a large turnover in the species pool with a limited effect on the functional diversity (e.g., Arctic $q = 2 - \text{MIS } 3$) (Villéger et al., 2010; Ibsen et al., 2020). In the context of climate change, shifts in ecosystem services as characterized by functional diversity are linked to shifts in taxonomic diversity but triggered differently. Functional diversity experienced fewer significant diversity shifts than taxonomic diversity, highlighting the possibility of increased resilience to environmental change. Functional diversity shifts occur both prior to and following species composition shifts, suggesting uncertainty in predicting responses to future climate change. As with taxonomic diversity, regional history plays the most important role in determining the degree to which functional diversity, and by extension ecosystem services, may be affected by climate change.

Regional climate

We expected diversity to increase with distance from the continental ice sheets based on compression of latitudinal temperature gradients. Changes in expected diversity should reflect admixtures of regional floras as they responded to shifts in temperature based on individualistic response of taxa to climate (Bartlein et al., 1986; Minckley et al., 2019). However, our results show regional responses to global temperature changes are difficult to predict due to mismatches between regional and global climate variability. Significant shifts happened since the last interglacial, but not proximal to MIS boundaries (Figs. 3–5). Age uncertainties and sampling resolution of older pollen records may create enough error in these records to blur direct mechanistic links between MIS transitions and regional vegetation changes. Previous studies have shown vegetation composition to reliably track climate at millennial scales (Harrison and Sanchez Goñi, 2010; Jiménez-Moreno et al., 2010a), but our results suggest major floral transitions represented by significant changes to pollen diversity lack a direct association with global climate shifts. This discrepancy is likely due to our incorporation of diversity metrics (qD and ${}^qD(Q)$) rather than focusing on dominant plant taxa. However, describing how correlated the two are to one another will be important for future studies. Regionally, changes in diversity are not uniform in magnitude or trend. In many cases, shifts observed in one region are not paralleled in the trends of another, even when geographically adjacent.

Understanding the role regional climate plays in influencing plant diversity has important implications for how we predict future diversity trends. The regional variability of diversity shifts is one of the difficulties revealed by our study. Plant diversity metrics (qD and ${}^qD(Q)$) for the Intermountain West indicate a high degree of stability over the last ca. 130 ka. Individual sites within the region experienced transitions between more open sagebrush steppe and closed spruce–fir forests in line with changes from warm–dry to cool–wet climates (Beiswenger, 1991; Herring and Gavin, 2015). Despite changes to its floral composition, the overall diversity of the Intermountain West remains relatively low compared to the rest of the continent, indicating that observed compositional shifts are relatively minor compared to more palynologically diverse regions (Fig. 6).

In contrast, the Yucatán, a diversity hotspot for North America, fluctuates more in trend with orders of $q = 1$ and $q = 2$ (Figs. 3–5).

While the lower diversity of the Intermountain West is partially a result of the biases of the pollen record with family-level pollen types (e.g., Poaceae, Asteraceae, Amaranthaceae) more common in the West than genus-level pollen types (e.g., *Betula*, *Tilia*, *Acer*, etc.) identified in eastern North American pollen records (Qian, 1998; Pinto-Ledezma et al., 2018; Cavender-Bares et al., 2020). With the flora of the Intermountain West adapted to grow in both hot and freezing arid conditions, changes to the temperature of the environment may not have been severe enough to shift the overall communities, but rather altered the latitudes and elevations that different communities could grow (Breshears et al., 2008; Lavin et al., 2013).

Diversity may tend to decrease into stadial periods and increase into interstadials, but this pattern is not universal (e.g., Mexico $q = 1 - \text{MIS } 4-2$). With the range of environmental conditions contained within the seven North American regions, it is difficult to determine external forcings outside of increased uniformity in hemispheric climate, possibly because of maritime effects. As with global temperature and atmospheric CO_2 , regional temperature ($\delta^{18}\text{O}$) alone does not explain all observed diversity shifts. Many instances exist where diversity increases with increasing temperature (e.g., Southeast $q = 0 - \text{MIS } 2-1$, Yucatán $q = 1 - \text{MIS } 2-1$, Mexico $q = 0 - \text{MIS } 4-3$) and decrease with decreasing temperature (e.g., Pacific Northwest $q = 0 - \text{MIS } 3-2$, Yucatán $q = 1 - \text{MIS } 5a-4$, Mexico $q = 0 - \text{MIS } 3-2$). Mismatches between both conditions occur, with scenarios of increasing diversity with decreasing temperature (e.g., Arctic $q = 0 - \text{MIS } 3$, Southeast $q = 1 - \text{MIS } 2$, Pacific Northwest $q = 0 - \text{MIS } 4$) and decreasing diversity with increasing temperature (e.g., Arctic $q = 0 - \text{MIS } 2-1$, Southeast $q = 1 - \text{MIS } 2-1$, Intermountain West $q = 0 - \text{MIS } 4-3$). While cooler temperatures do not correlate to lower diversity and vice versa (Scheiner and Rey-Benayas, 1994; Donoghue, 2008), the lack of clear patterns determining whether a decrease in temperature is associated with a diversity increase, decrease, or no change suggests other climatic factors play a major role. The most likely factor is moisture availability as it is an important environmental gradient for global plant niches (Silvertown, 2004). However, highly resolved paleohydrology records older than the last glacial period are not readily available, making explorations of this driver of past diversity for North America not currently possible. Regional temperature records align with plant diversity shifts to a better degree than global temperature, but again, without independent moisture data, continental diversity patterns cannot be fully explained. Increased research focusing on isotopic biomarkers (Seki et al., 2011; Feakins et al., 2016; Strobel et al., 2022) could result in the development of regionalized moisture records and complete the picture of regional climates during the last interglacial–glacial cycle.

Conclusions

The reconstructions of geographic and temporal shifts in plant diversity outline the continental dynamics of vegetation over the last ~130 ka. We examined changes in floristic diversity of the past 130 ka (MIS 5e–MIS 1) using 23 pollen records from North America via the implementation of Hill numbers, allowing for a simultaneous examination of species richness and FAD based on presence-absence (orders of $q = 0$), rarity (orders of $q = 1$), or dominance (orders of $q = 2$). Both Shannon's (1D) and functional Shannon's indices (${}^1D(Q)$) and Simpson's (2D) and Gini–Simpson's indices (${}^2D(Q)$) fluctuate to a higher degree than richness (0D)

and FAD (${}^0D(Q)$), indicating that the compositions within ecosystems were highly variable across the record, while species pools remained relatively constant.

The incorporation of functional diversity (${}^qD(Q)$) alongside taxonomic diversity (qD) supported our interpretations of diversity dynamics during the last interglacial–glacial cycle and shows the connectivity between the two metrics. However, desynchronies between taxonomic and functional diversity shifts point to differences in resilience between species composition and ecosystem function. Continued mechanistic investigations into individual region shifts in both taxonomic and functional plant diversity can identify relationships between global climate and regional vegetation to further understand Quaternary plant dynamics.

Our results highlight the relationship between global temperature, regional climate, ecosystem function, and species composition. While shifts in global temperature may correspond with shifts in the regional climate, how plant diversity and the broader ecosystem respond is unpredictable. However, the integration of both taxonomic and functional diversity into our study emphasizes the inseparability between the two. Scenarios exist in which one metric experiences a shift prior to or without the other, yet both maintain similar temporal and spatial patterns to one another throughout the cooling and warming cycles of the last 130 ka.

Supplementary material. The supplementary material for this article can be found at <https://doi.org/10.1017/qua.2024.55>.

Acknowledgments. We thank the contributors to the Neotoma Paleocology Database (<https://www.neotomadb.org/>) and the following data contributors for enabling this compilation to be possible: Thomas Ager, Patricia Anderson, Scott Anderson, Jane Beiswenger, Alexander Correa-Metrio, Les Cwynar, Paul Delcourt, Bianca Frechette, Katherine Glover, Laurie Grigg, Eric Grimm, Barbara Hansen, Katharine Hakala, Erin Herring, Calvin Heusser, Bonnie Fine Jacobs, Gonzalo Jiménez-Moreno, Matthew Kirby, Glen MacDonald, John McAndrews, Robert Thompson, Charles Turton, William Watts, Cathy Whitlock, Marjorie Green Winkler, and Mark Worona. In addition, we thank BIEN (<https://bien.nceas.ucsb.edu/bien/>) and the hundreds of individuals and herbaria whose trait observations and measurements were used in our functional diversity estimates. We thank the University of Wyoming Roy J. Shlemon Center for Quaternary Studies for providing financial support. We appreciate the anonymous reviewers whose comments helped improve this work. We are grateful for the contributions of Simon Brewer, providing code and recommendations in our analyses. Map generation for Figs. 1 and 6 was possible with the help of John Lesko.

Data availability statement. Datasets and R code related to this study can be found at: https://github.com/tjterlizzi/NA_diversity.git.

Funding. This work was supported by the Roy J. Shlemon Center for Quaternary Studies at the University of Wyoming. The center had no involvement in the development or execution of the research.

References

- Ager, T.A., 2003. Late Quaternary vegetation and climate history of the central Bering land bridge from St. Michael Island, western Alaska. *Quaternary Research* **60**, 19–32.
- Anderson, P.M., 1988. Late Quaternary pollen records from the Kobuk and Noatak River drainages, northwestern Alaska. *Quaternary Research* **29**, 263–276.
- Bailey, R.G., 2014. *Ecoregions: The Ecosystem Geography of the Oceans and Continents*, 2nd ed. New York, Springer.
- Barnosky, A.D., Hadly, E.A., Gonzalez, P., Head, J., Polly, P.D., Lawing, A.M., Eronen, J.T., et al., 2017. Merging paleobiology with conservation biology to guide the future of terrestrial ecosystems. *Science* **355**, eaah4787. <https://doi.org/10.1126/science.aah4787>
- Bartlein, P.J., Anderson, K.H., Anderson, P.M., Edwards, M.E., Mock, C.J., Thompson, R.S., Webb, R.S., Whitlock, C., 1998. Paleoclimate simulations for North America over the past 21,000 years: features of the simulated climate and comparisons with paleoenvironmental data. *Quaternary Science Reviews* **17**, 549–585.
- Bartlein, P.J., Prentice, I.C., Webb, T., 1986. Climatic response surfaces from pollen data for some Eastern North-American taxa. *Journal of Biogeography* **13**, 35–57.
- Batchelor, C.L., Margold, M., Krapp, M., Murton, D.K., Dalton, A.S., Gibbard, P.L., Stokes, C.R., Murton, J.B., A. Manica, A., 2019. The configuration of Northern Hemisphere ice sheets through the Quaternary. *Nature Communications* **10**, 3713. <https://doi.org/10.1038/s41467-019-11601-2>
- Beiswenger, J.M., 1991. Late Quaternary vegetational history of Grays Lake, Idaho. *Ecological Monographs* **61**, 165–182.
- Benton, M.J., 2009. The Red Queen and the Court Jester: species diversity and the role of biotic and abiotic factors through time. *Science* **323**, 728–732.
- Bereiter, B., Eggleston, S., Schmitt, J., Nehrbass-Ahles, C., Stocker, T.F., Fischer, H., Kipfstuhl, S., Chappellaz, J., 2015. Revision of the EPICA Dome C CO₂ record from 800 to 600 kyr before present. *Geophysical Research Letters* **42**, 542–549. <https://doi.org/10.1002/2014GL061957>
- Birks, H.H., Birks, H.J.B., 2000. Future uses of pollen analysis must include plant macrofossils. *Journal of Biogeography* **27**, 31–35.
- Birks, H.J.B., 2019. Contributions of Quaternary botany to modern ecology and biogeography. *Plant Ecology & Diversity* **12**, 189–385.
- Birks, H.J.B., Felde, V.A., Bjure, A.E., Grytnes, J.-A., Seppä, H., Giesecke, T., 2016. Does pollen-assembly richness reflect floristic richness? A review of recent developments and future challenges. *Review of Palaeobotany and Palynology* **228**, 1–25.
- Breshears, D.D., Huxman, T.E., Adams, H.D., Zou, C.B., Davison, J.E., 2008. Vegetation synchronously leans upslope as climate warms. *Proceedings of the National Academy of Sciences* **105**, 11591–11592.
- Brussel, T., Brewer, S.C., 2021. Functional Paleocology and the Pollen-Plant Functional Trait Linkage. *Frontiers in Ecology and Evolution* **8**, 564609. <https://doi.org/10.3389/fevo.2020.564609>
- Cavender-Bares, J., Schweiger, A.K., Pinto-Ledezma, J.N., Meireles, J.E., 2020. Applying remote sensing to biodiversity science. In: Cavender-Bares, J., Gamon, J.A., Townsend, P.A. (Eds.), *Remote Sensing of Plant Biodiversity*. Springer International Publishing, Cham, Switzerland, pp. 13–42.
- CEC [Commission for Environmental Cooperation], 1997. *Ecological Regions of North America: Toward a Common Perspective*. Communications and Public Outreach Department of the CEC Secretariat, Montréal, 71 pp. <http://www.cec.org/files/documents/publications/1701-ecological-regions-north-america-toward-common-perspective-en.pdf>
- Chacón-Labela, J., Hinojo-Hinojo, C., Bohner, T., Castorena, M., Violle, C., Vandvik, V., Enquist, B.J., 2023. How to improve scaling from traits to ecosystem processes. *Trends in Ecology & Evolution* **38**, 228–237.
- Chao, A., Chiu, C.-H., Jost, L., 2014a. Unifying species diversity, phylogenetic diversity, functional diversity, and related similarity and differentiation measures through Hill numbers. *Annual Review of Ecology, Evolution, and Systematics* **45**, 297–324.
- Chao, A., Gotelli, N.J., Hsieh, T.C., Sander, E.L., Ma, K.H., Colwell, R.K., Ellison, A.M., 2014b. Rarefaction and extrapolation with Hill numbers: a framework for sampling and estimation in species diversity studies. *Ecological Monographs* **84**, 45–67.
- Cheddadi, R., de Beaulieu, J.-L., Jouzel, J., Andrieu-Ponel, V., Laurent, J.-M., Reille, M., Raynaud, D., Bar-Hen, A., 2005. Similarity of vegetation dynamics during interglacial periods. *Proceedings of the National Academy of Sciences* **102**, 13939–13943.
- Chiu, C.-H., Chao, A., 2014. Distance-based functional diversity measures and their decomposition: a framework based on Hill numbers. *PLoS ONE* **9**, e100014. <https://doi.org/10.1371/journal.pone.0100014>
- Cleal, C., Pardoe, H.S., Berry, C.M., Cascales-Miñana, B., Davis, B.A.S., Diez, J.B., Filipova-Marinova, M.V., et al., 2021. Palaeobotanical experiences of plant diversity in deep time. 1: How well can we identify past plant diversity in the fossil record? *Palaeogeography, Palaeoclimatology, Palaeoecology* **576**, 110481. <https://doi.org/10.1016/j.palaeo.2021.110481>
- Colman, S.M., Kaufman, D., Bright, J., Heil, C., King, J., Dean, W., Rosenbaum, J., Forester, R., Bischoff, J., Perkins, M., 2006. Age model

- for a continuous, ca 250-ka Quaternary lacustrine record from Bear Lake, Utah–Idaho. *Quaternary Science Reviews* **25**, 2271–2282.
- Comes, H.P., Kadereit, J.W.**, 1998. The effect of Quaternary climatic changes on plant distribution and evolution. *Trends in Plant Science* **3**, 432–438.
- Correa-Metrio, A., Bush, M.B., Cabrera, K.R., Sully, S., Brenner, M., Hodell, D.A., Escobar, J., Guilderson, T.**, 2012. Rapid climate change and no-analog vegetation in lowland Central America during the last 86,000 years. *Quaternary Science Reviews* **38**, 63–75.
- Correa-Metrio, A., Bush, M.B., Hodell, D.A., Brenner, M., Escobar, J., Guilderson, T.**, 2012. The influence of abrupt climate change on the ice-age vegetation of the Central American lowlands. *Journal of Biogeography* **39**, 497–509. <https://doi.org/10.1111/j.1365-2699.2011.02618.x>
- Cronin, T.M., Keller, K.J., Farmer, J.R., Schaller, M.F., O'Regan, M., Poirier, R., Coxall, H., Dwyer, G.S., Bauch, H., I. G. Kindstedt**, 2019. Interglacial paleoclimate in the Arctic. *Paleoceanography and Paleoclimatology* **34**, 1959–1979.
- Cutler, K., Edwards, R., Taylor, F., Cheng, H., Adkins, J., Gallup, C., Cutler, P., Burr, G., Bloom, A.**, 2003. Rapid sea-level fall and deep-ocean temperature change since the last interglacial period. *Earth and Planetary Science Letters* **206**, 253–271.
- Cwynar, L.C.**, 1982. A late-Quaternary vegetation history from Hanging Lake, northern Yukon. *Ecological Monographs* **52**, 1–24.
- Dakos, V., Matthews, B., Hendry, A.P., Levine, J., Loeuille, N., Norberg, J., Nosil, P., Scheffer, M., De Meester, L.**, 2019. Ecosystem tipping points in an evolving world. *Nature Ecology & Evolution* **3**, 355–362.
- Davis, M.B., Shaw, R.G.**, 2001. Range shifts and adaptive responses to Quaternary climate change. *Science* **292**, 673–679.
- Delcourt, P.A., Delcourt, H.R., Brister, R.C., Lackey, L.E.**, 1980. Quaternary vegetation history of the Mississippi Embayment 1, 2. *Quaternary Research* **13**, 111–132.
- Donoghue, M.J.**, 2008. A phylogenetic perspective on the distribution of plant diversity. *Proceedings of the National Academy of Sciences* **105**, 11549–11555.
- Doxa, A., Devictor, V., Baumel, A., Pavon, D., Medail, F., Leriche, A.**, 2020. Beyond taxonomic diversity: revealing spatial mismatches in phylogenetic and functional diversity facets in Mediterranean tree communities in southern France. *Forest Ecology and Management* **474**, 118318. <https://doi.org/10.1016/j.foreco.2020.118318>.
- Eronen, J.T., Polly, P.D., Fred, M., Damuth, J., Frank, D.C., Mosbrugger, V., Scheidegger, C., Stenseth, N.C., Fortelius, M.**, 2010. Ecometrics: the traits that bind the past and present together. *Integrative Zoology* **5**, 88–101.
- Feakins, S.J., Bentley, L.P., Salinas, N., Shenkin, A., Blonder, B., Goldsmith, G.R., Ponton, C., et al.**, 2016. Plant leaf wax biomarkers capture gradients in hydrogen isotopes of precipitation from the Andes and Amazon. *Geochimica et Cosmochimica Acta* **182**, 155–172.
- Felde, V.A., Peglar, S.M., Bjune, A.E., Grytnes, J.-A., Birks, H.J.B.**, 2016. Modern pollen–plant richness and diversity relationships exist along a vegetational gradient in southern Norway. *The Holocene* **26**, 163–175.
- Felde, V.A., Flantua, S.G.A., Jenks, C.R., Benito, B.M., de Beaulieu, J.-L., Kuneš, P., Magri, D., et al.**, 2020. Compositional turnover and variation in Eemian pollen sequences in Europe. *Vegetation History and Archaeobotany* **29**, 101–109.
- Fréchette, B., Wolfe, A.P., Miller, G.H., Richard, P.J., de Vernal, A.**, 2006. Vegetation and climate of the last interglacial on Baffin Island, Arctic Canada. *Paleoceanography, Palaeoclimatology, Palaeoecology* **236**, 91–106.
- Fréchette, B., de Vernal, A., Richard, P.J.**, 2008. Holocene and last interglacial cloudiness in eastern Baffin Island, Arctic Canada. *Canadian Journal of Earth Sciences* **45**, 1221–1234.
- Gentry, A.H.**, 1988. Changes in plant community diversity and floristic composition on environmental and geographical gradients. *Annals of the Missouri Botanical Garden* **75**, 1–34.
- Glover, K.C., MacDonald, G.M., Kirby, M.E., Rhodes, E.J., Stevens, L., Silveira, E., Whitaker, A., Lydon, S.**, 2017. Evidence for orbital and North Atlantic climate forcing in alpine Southern California between 125 and 10 ka from multi-proxy analyses of Baldwin Lake. *Quaternary Science Reviews* **167**, 47–62.
- Glover, K.C., Chaney, A., Kirby, M.E., Patterson, W.P., MacDonald, G.M.**, 2020. Southern California vegetation, wildfire, and erosion had nonlinear responses to climatic forcing during marine isotope stages 5–2 (120–15 ka). *Paleoceanography and Paleoclimatology* **35**, e2019PA003628. <https://doi.org/10.1029/2019PA003628>
- Glover, K.C., George, J., Heusser, L., MacDonald, G.M.**, 2021. West Coast vegetation shifts as a response to climate change over the past 130,000 years: geographic patterns and process from pollen data. *Physical Geography* **42**, 542–560.
- Godfray, H.C.J., Knapp, S., Forey, P.L., Fortey, R.A., Kenrick, P., Smith, A.B.**, 2004. Taxonomy and fossils: a critical appraisal. *Philosophical Transactions of the Royal Society of London. Series B: Biological Sciences* **359**, 639–653.
- Goring, S., Lacourse, T., Pellatt, M.G., Mathewes, R.W.**, 2013. Pollen assemblage richness does not reflect regional plant species richness: a cautionary tale. *Journal of Ecology* **101**, 1137–1145.
- Griffith, G.E., Omernik, J.M., Azevedo, S.H.**, 1998. *Ecological Classification of the Western Hemisphere*. A report to Thomas R. Loveland, project manager EROS Data Center, U.S. Geological Survey, Sioux Falls, SD.
- Grigg, L.D., Whitlock, C.**, 2002. Patterns and causes of millennial-scale climate change in the Pacific Northwest during Marine Isotope stages 2 and 3. *Quaternary Science Reviews* **21**, 2067–2083.
- Grimm, E.C., Watts, W.A., Jacobson, G.L., Hansen, B.C.S., Almquist, H.R., Dieffenbacher-Krall, A.C.**, 2006. Evidence for warm wet Heinrich events in Florida. *Quaternary Science Reviews* **25**, 2197–2211.
- Guiot, J., de Beaulieu, J.L., Cheddadi, R., David, F., Ponel, P., Reille, M.**, 1993. The climate in Western Europe during the last glacial/interglacial cycle derived from pollen and insect remains. *Palaeogeography, Palaeoclimatology, Palaeoecology* **103**, 73–93.
- Hakala, K.J., Adam, D.P.**, 2004. Late Pleistocene vegetation and climate in the southern Cascade Range and the Modoc Plateau region. *Journal of Paleolimnology* **31**, 189–215.
- Harrison, S.P., Sanchez Goñi, M.F.**, 2010. Global patterns of vegetation response to millennial-scale variability and rapid climate change during the last glacial period. *Quaternary Science Reviews* **29**, 2957–2980.
- Hector, A., Schmid, B., Beierkuhnlein, C., Caldeira, M.C., Diemer, M., Dimitrakopoulos, P.G., Finn, J.A., et al.**, 1999. Plant diversity and productivity experiments in European grasslands. *Science* **286**, 1123–1127.
- Helmens, K.F.**, 2014. The last interglacial–glacial cycle (MIS 5–2) re-examined based on long proxy records from central and northern Europe. *Quaternary Science Reviews* **86**, 115–143.
- Hendy, I., Minkley, T., Whitlock, C.**, 2016. Eastern tropical Pacific vegetation response to rapid climate change and sea level rise: a new pollen record from the Gulf of Tehuantepec, southern Mexico. *Quaternary Science Reviews* **145**, 152–160.
- Herbert, T., Schuffert, J., Andreassen, D., Heusser, L., Lyle, M., Mix, A., Ravelo, A., Stott, L., Herguera, J.**, 2001. Collapse of the California Current during glacial maxima linked to climate change on land. *Science* **293**, 71–76.
- Herring, E.M., Gavin, D.G.**, 2015. Climate and vegetation since the last interglacial (MIS 5e) in a putative glacial refugium, northern Idaho, USA. *Quaternary Science Reviews* **117**, 82–95.
- Heusser, C.J.**, 1972. Palynology and phytogeographical significance of a late-Pleistocene refugium near Kalaloch, Washington. *Quaternary Research* **2**, 189–201.
- Holland, S.M.**, 2008. Detrended correspondence analysis (DCA). <http://stratigrafia.org/fieldconference/tutorials/R-DCATutorial.pdf> (20 August, 2009)
- Howard, L.F., Lee, T.D.**, 2003. Temporal patterns of vascular plant diversity in southeastern New Hampshire forests. *Forest Ecology and Management* **185**, 5–20.
- Ibsen, P.C., Borowy, D., Rochford, M., Swan, C.M., Jenerette, G.D.**, 2020. Influence of climate and management on patterns of taxonomic and functional diversity of recreational park vegetation. *Frontiers in Ecology and Evolution* **8**, 501502. <https://doi.org/10.3389/fevo.2020.501502>
- Isbell, F., Calcagno, V., Hector, A., Connolly, J., Harpole, W.S., Reich, P.B., Scherer-Lorenzen, M., et al.**, 2011. High plant diversity is needed to maintain ecosystem services. *Nature* **477**, 199–202.
- Jacobs, B.F.**, 1985. A middle Wisconsin pollen record from Hay Lake, Arizona. *Quaternary Research* **24**, 121–130.

- Jiménez-Moreno, G., Anderson, R.S., Fawcett, P.J., 2007. Orbital- and millennial-scale vegetation and climate changes of the past 225 ka from Bear Lake, Utah–Idaho (USA). *Quaternary Science Reviews* **26**, 1713–1724.
- Jiménez-Moreno, G., Anderson, R.S., Desprat, S., Grigg, L.D., Grimm, E.C., Heusser, L.E., Jacobs, B.F., López-Martínez, C., Whitlock, C.L., Willard, D.A., 2010a. Millennial-scale variability during the last glacial in vegetation records from North America. *Quaternary Science Reviews* **29**, 2865–2881.
- Jiménez-Moreno, G., Fauquette, G., Suc, J.-P., 2010b. Miocene to Pliocene vegetation reconstruction and climate estimates in the Iberian Peninsula from pollen data. *Review of Palaeobotany and Palynology* **162**, 403–415.
- Jost, L., 2006. Entropy and diversity. *Oikos* **113**, 363–375.
- Jost, L., 2007. Partitioning diversity into independent alpha and beta components. *Ecology* **88**, 2427–2439.
- Krivoruchko, K., 2012. Empirical bayesian kriging. *ArcUser Fall* **6**, 1145. <https://www.esri.com/news/arcuser/1012/empirical-bayesian-kriging.html>
- Lamanna, C., Blonder, B., Violle, C., Kraft, N.J.B., Sandel, B., Šimová, I., Donoghue, J.C., et al., 2014. Functional trait space and the latitudinal diversity gradient. *Proceedings of the National Academy of Sciences* **111**, 13745–13750.
- Lavin, M., Brummer, T.J., Quire, R., Maxwell, B.D., Rew, L.J., 2013. Physical disturbance shapes vascular plant diversity more profoundly than fire in the sagebrush steppe of southeastern Idaho, U.S.A. *Ecology and Evolution* **3**, 1626–1641.
- Lisiecki, L.E., Raymo, M.E., 2005. A Pliocene–Pleistocene stack of 57 globally distributed benthic $\delta^{18}\text{O}$ records. *Paleoceanography* **20**, PA1003. <https://doi.org/10.1029/2004PA001071>
- López-Angulo, J., Pescador, D.S., Sánchez, A.M., Luzuriaga, A.L., Cavieres, L.A., Escudero, A., 2020. Impacts of climate, soil and biotic interactions on the interplay of the different facets of alpine plant diversity. *Science of The Total Environment* **698**, 133960. <https://doi.org/10.1016/j.scitotenv.2019.133960>
- Lucchi, M.R., 2008. Vegetation dynamics during the last interglacial–glacial cycle in the Arno coastal plain (Tuscany, western Italy): location of a new tree refuge. *Quaternary Science Reviews* **27**, 2456–2466.
- Maitner, B.S., Boyle, B., Casler, N., Condit, R., Donoghue, J., II, Durán, S.M., Guaderrama, D., et al., 2018. The bien r package: a tool to access the Botanical Information and Ecology Network (BIEN) database. *Methods in Ecology and Evolution* **9**, 373–379.
- Matthias, I., Semmler, M.S.S., Giesecke, T., 2015. Pollen diversity captures landscape structure and diversity. *Journal of Ecology* **103**, 880–890.
- Miller, G.H., Wolfe, A.P., Steig, E.J., Sauer, P.E., Kaplan, M.R., Briner, J.P., 2002. The Goldilocks dilemma: big ice, little ice, or “just-right” ice in the eastern Canadian Arctic. *Quaternary Science Reviews* **21**, 33–48.
- Minckley, T.A., Felstead, N.J., Gonzalez, S., 2019. Novel vegetation and establishment of Chihuahuan Desert communities in response to late Pleistocene moisture availability in the Cuatrociénegas Basin, NE Mexico. *The Holocene* **29**, 457–466.
- Minckley, T.A., Clementz, M.T., Kornfeld, M., Larson, M.L., Finley, J., 2021. Late Pleistocene environments of the Bighorn Basin, Wyoming–Montana, USA. *Quaternary Research* **99**, 128–141.
- Minckley, T.A., Clementz, M.T., Lovelace, D., 2023. Paleo-vegetation and environmental history of Natural Trap Cave based on pollen and carbon isotope analyses. *Quaternary International* **647**, 103–111.
- Morris, E.K., Caruso, T., Buscot, F., Fischer, M., Hancock, C., Maier, T.S., Meiners, T., et al., 2014. Choosing and using diversity indices: insights for ecological applications from the German Biodiversity Exploratories. *Ecology and Evolution* **4**, 3514–3524.
- Ohlmann, M., Miele, V., Dray, S., Chalmandrier, L., O’Connor, L., Thuiller, W., 2019. Diversity indices for ecological networks: a unifying framework using Hill numbers. *Ecology Letters* **22**, 737–747.
- Oksanen, J., Blanchet, F.G., Kindt, R., Legendre, P., Minchin, P.R., O’hara, R., Simpson, G.L., Solymos, P., Stevens, M.H.H., Wagner, H., 2013. Package ‘vegan’. Community ecology package, version 2. <https://cran.r-project.org/web/packages/vegan/vegan.pdf>
- Pérez-Harguindeguy, N., Díaz, S., Garnier, E., Lavorel, S., Poorter, H., Jaureguiberry, P., Bret-Harte, M.S., et al., 2016. Corrigendum to: new handbook for standardised measurement of plant functional traits worldwide. *Australian journal of Botany* **64**, 715–716.
- Pinto-Ledezma, J.N., Larkin, D.J., Cavender-Bares, J., 2018. Patterns of beta diversity of vascular plants and their correspondence with biome boundaries across North America. *Frontiers in Ecology and Evolution* **6**, 194. <https://doi.org/10.3389/fevo.2018.00194>
- Qian, H., 1998. Large-scale biogeographic patterns of vascular plant richness in North America: an analysis at the generic level. *Journal of Biogeography* **25**, 829–836.
- Rao, C.R., 1982. Diversity and dissimilarity coefficients: a unified approach. *Theoretical Population Biology* **21**, 24–43.
- Reitalu, T., Bjune, A.E., Blaus, A., Giesecke, T., Helm, A., Matthias, I., Peglar, S.M., et al., 2019. Patterns of modern pollen and plant richness across northern Europe. *Journal of Ecology* **107**, 1662–1677.
- Ricketts, T.H., Dinerstein, E., Olsen, D.M., Loucks, C.J., Eichbaum, W., DellaSalla, D., Kavanagh, K., et al., 1999. *Terrestrial Ecoregions of North America: A Conservation Assessment*. Island Press, Washington, D.C.
- Roscher, C., Schumacher, J., Gubsch, M., Lipowsky, A., Weigelt, A., Buchmann, N., Schulze, E.-D., Schmid, B., 2018. Interspecific trait differences rather than intraspecific trait variation increase the extent and filling of community trait space with increasing plant diversity in experimental grasslands. *Perspectives in Plant Ecology, Evolution and Systematics* **33**, 42–50.
- Sax, D.F., Gaines, S.D., 2003. Species diversity: from global decreases to local increases. *Trends in Ecology & Evolution* **18**, 561–566.
- Scheiner, S.M., Rey-Benayas, J.M., 1994. Global patterns of plant diversity. *Evolutionary Ecology* **8**, 331–347.
- Schmidt, M.W., Spero, H.J., Lea, D.W., 2004. Links between salinity variation in the Caribbean and North Atlantic thermohaline circulation. *Nature* **428**, 160–163.
- Schuler, T.M., Gillespie, A.R., 2000. Temporal patterns of woody species diversity in a Central Appalachian forest from 1856 to 1997. *The Journal of the Torrey Botanical Society* **127**, 149–161.
- Seki, O., Meyers, P.A., Yamamoto, S., Kawamura, K., Nakatsuka, T., Zhou, W., Zheng, Y., 2011. Plant-wax hydrogen isotopic evidence for postglacial variations in delivery of precipitation in the monsoon domain of China. *Geology* **39**, 875–878.
- Silvertown, J., 2004. Plant coexistence and the niche. *Trends in Ecology & Evolution* **19**, 605–611.
- Simpson, G.L., 2018. Modelling palaeoecological time series using generalised additive models. *Frontiers in Ecology and Evolution* **6**, 149. <https://doi.org/10.3389/fevo.2018.00149>.
- Sotomayor, G., Hampel, H., Vázquez, R.F., Forio, M.A.E., Goethals, P.L.M., 2022. Implications of macroinvertebrate taxonomic resolution for freshwater assessments using functional traits: The Paute River Basin (Ecuador) case. *Diversity and Distributions* **28**, 1735–1747.
- Stohlgren, T.J., Owen, A.J., Lee, M., 2000. Monitoring shifts in plant diversity in response to climate change: a method for landscapes. *Biodiversity & Conservation* **9**, 65–86.
- Strobel, P., Bliedtner, M., Carr, A.S., Struck, J., du Plessis, N., Glaser, B., Meadows, M.E., et al., 2022. Reconstructing Late Quaternary precipitation and its source on the southern Cape coast of South Africa: a multiproxy paleoenvironmental record from Vankervelsvlei. *Quaternary Science Reviews* **284**, 107467. <https://doi.org/10.1016/j.quascirev.2022.107467>.
- Suggitt, A.J., Lister, D.G., Thomas, C.D., 2019. Widespread effects of climate change on local plant diversity. *Current Biology* **29**, 2905–2911.e2902. <https://doi.org/10.1016/j.cub.2019.06.079>
- Tausch, R., Wigand, P.E., Burkhardt, J.W., 1993. Viewpoint: plant community thresholds, multiple steady states, and multiple successional pathways: legacy of the Quaternary? *Journal of Range Management* **46**, 439–447.
- ter Braak, C.J.F., Prentice, I.C., 2004. A theory of gradient analysis. *Advances in Ecological Research* **18**, 271–317.
- Thompson, R.S., 1992. Late Quaternary environments in Ruby Valley, Nevada. *Quaternary Research* **37**, 1–15.
- Thuiller, W., Lavorel, S., Araújo, M.B., Sykes, M.T., Prentice, I.C., 2005. Climate change threats to plant diversity in Europe. *Proceedings of the National Academy of Sciences* **102**, 8245–8250.
- Tilman, D., Lehman, C.L., Thomson, K.T., 1997. Plant diversity and ecosystem productivity: theoretical considerations. *Proceedings of the National Academy of Sciences* **94**, 1857–1861.

- Tzedakis, P.C., Raynaud, D., McManus, J.F., Berger, A., Brovkin, V., Kiefer, T.**, 2009. Interglacial diversity. *Nature Geoscience* **2**, 751–755.
- Väli, V., Odgaard, B.V., Väli, Ü., Poska, A.**, 2022. Pollen richness: a reflection of vegetation diversity or pollen-specific parameters? *Vegetation History and Archaeobotany* **31**, 611–622.
- van der Knaap, W.O.**, 2009. Estimating pollen diversity from pollen accumulation rates: a method to assess taxonomic richness in the landscape. *The Holocene* **19**, 159–163.
- Villéger, S., Miranda, J.R., Hernández, D.F., Mouillot, D.**, 2010. Contrasting changes in taxonomic vs. functional diversity of tropical fish communities after habitat degradation. *Ecological Applications* **20**, 1512–1522.
- von Humboldt, A., Bonpland, A.**, 2010. *Essay on the Geography of Plants*. University of Chicago Press, Chicago.
- Watts, W.A., Bradbury, J.P.**, 1982. Paleoeological studies at Lake Patzcuaro on the west-central Mexican Plateau and at Chalco in the Basin of Mexico. *Quaternary Research* **17**, 56–70.
- Weng, C., Hooghiemstra, H., Duivenvoorden, J.F.**, 2006. Challenges in estimating past plant diversity from fossil pollen data: statistical assessment, problems, and possible solutions. *Diversity and Distributions* **12**, 310–318.
- Westoby, M.**, 1998. A leaf-height-seed (LHS) plant ecology strategy scheme. *Plant and Soil* **199**, 213–227.
- Whitlock, C., Sarna-Wojcicki, A.M., Bartlein, P.J., Nickmann, R.J.**, 2000. Environmental history and tephrostratigraphy at Carp Lake, southwestern Columbia Basin, Washington, USA. *Palaeogeography Palaeoclimatology Palaeoecology* **155**, 7–29.
- Wilcox, P.S., Honiat, C., Trüssel, M., Edwards, R.L., Spötl, C.**, 2020. Exceptional warmth and climate instability occurred in the European Alps during the last interglacial period. *Communications Earth & Environment* **1**, 57. <https://doi.org/10.1038/s43247-020-00063-w>
- Williams, J.W., B. Shuman, B.N., Webb, T., III, Bartlein, P.J., Leduc, P.L.**, 2004. Late-Quaternary vegetation dynamics in North America: scaling from taxa to biomes. *Ecological Monographs* **74**, 309–334.
- Williams, J.W., Grimm, E.C., Blois, J.L., Charles, D.F., Davis, E.B., Goring, S.J., Graham, R.W., Smith, A.J., Anderson, M., Arroyo-Cabrales, J.**, 2018. The Neotoma Paleocology Database, a multiproxy, international, community-curated data resource. *Quaternary Research* **89**, 156–177.
- Willis, K.J., Bailey, R.M., Bhagwat, S.A., Birks, H.J.B.**, 2010. Biodiversity baselines, thresholds and resilience: testing predictions and assumptions using palaeoecological data. *Trends in Ecology & Evolution* **25**, 583–591.
- Wohlfarth, B.**, 2013. *A Review of Early Weichselian Climate (MIS 5d–a) in Europe*. Technical Report TR-13-03, Svensk Kärnbränslehantering AB, Swedish Nuclear Fuel and Waste Management Co., Stockholm, Sweden, 79 pp.
- Wolfe, A.P., Frechette, B., Richard, P.J., Miller, G.H., Forman, S.L.**, 2000. Paleocology of a > 90,000-year lacustrine sequence from Fog Lake, Baffin Island, Arctic Canada. *Quaternary Science Reviews* **19**, 1677–1699.
- Wood, S.N.**, 2001. mgcv: GAMs and generalized ridge regression for R. *R news* **1**, 20–25.
- Worona, M.A., Whitlock, C.**, 1995. Late Quaternary vegetation and climate history near Little Lake, central Coast Range, Oregon. *Geological Society of America Bulletin* **107**, 867–876.
- Zak, D.R., Holmes, W.E., White, D.C., Peacock, A.D., Tilman, D.**, 2003. Plant diversity, soil microbial communities, and ecosystem function: are there any links? *Ecology* **84**, 2042–2050.